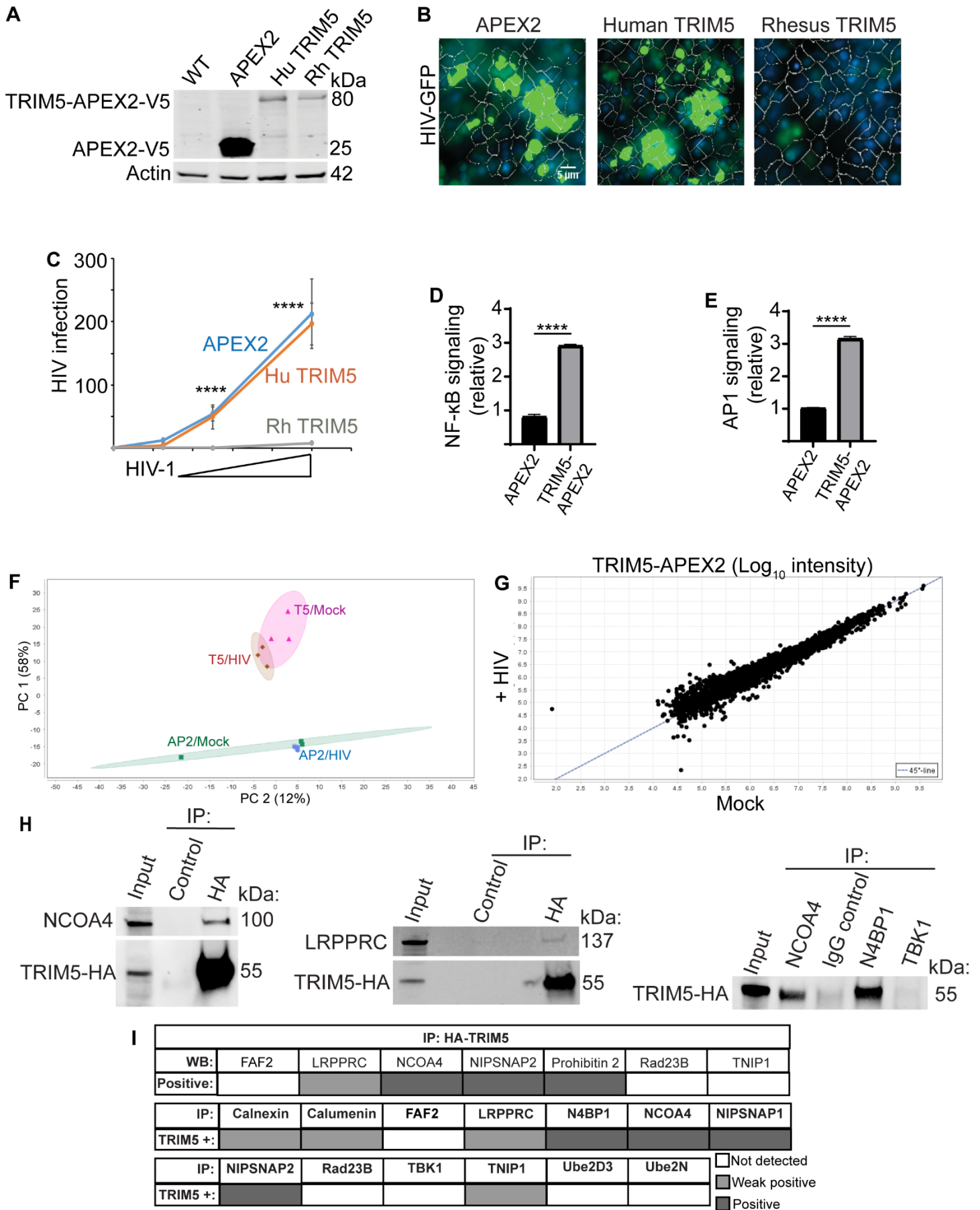


**Cell Reports, Volume 39**

**Supplemental information**

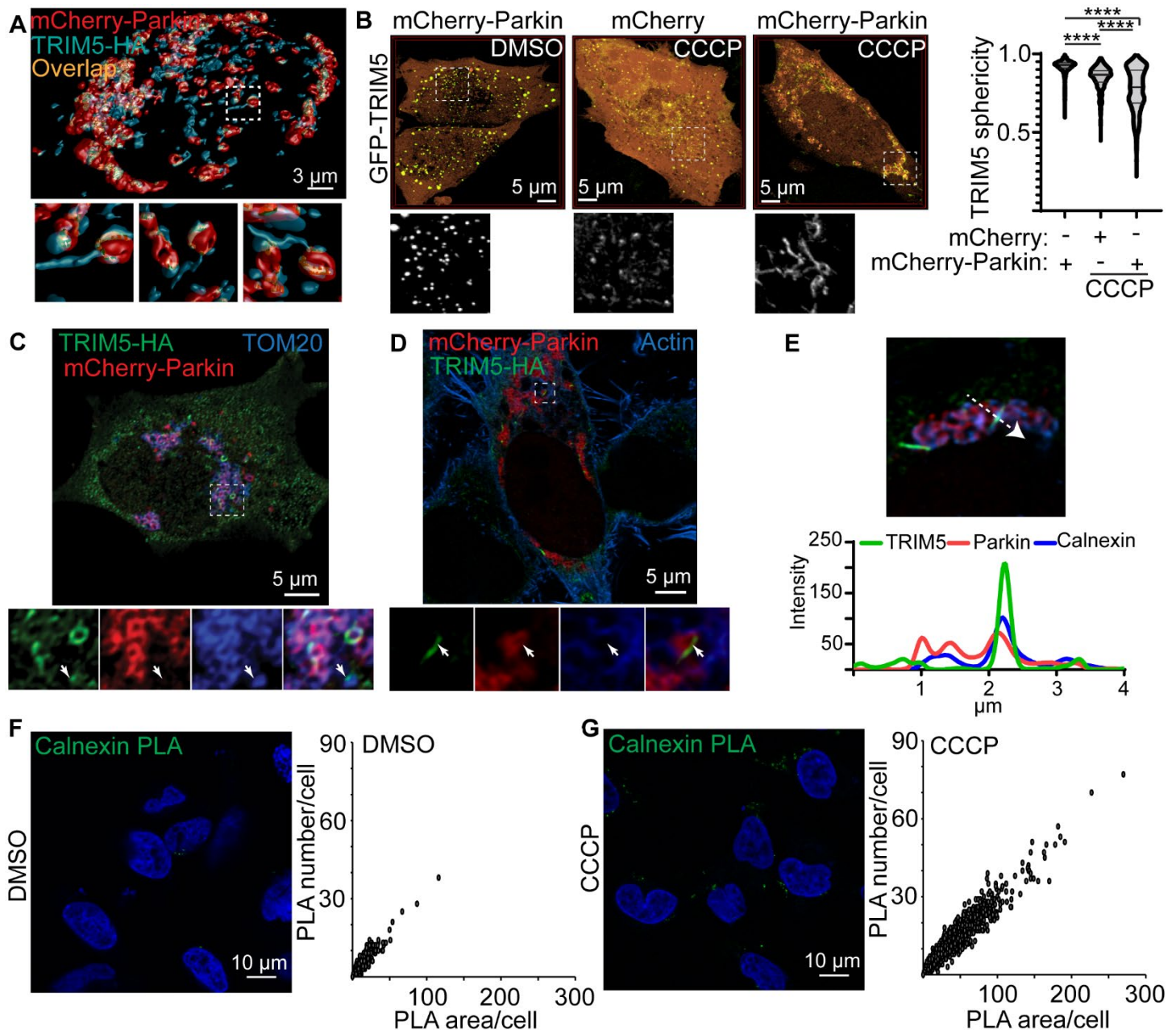
**Interactomic analysis reveals  
a homeostatic role for the HIV  
restriction factor TRIM5 $\alpha$  in mitophagy**

**Bhaskar Saha, Michelle Salemi, Geneva L. Williams, Seun Oh, Michael L. Paffett, Brett Phinney, and Michael A. Mandell**



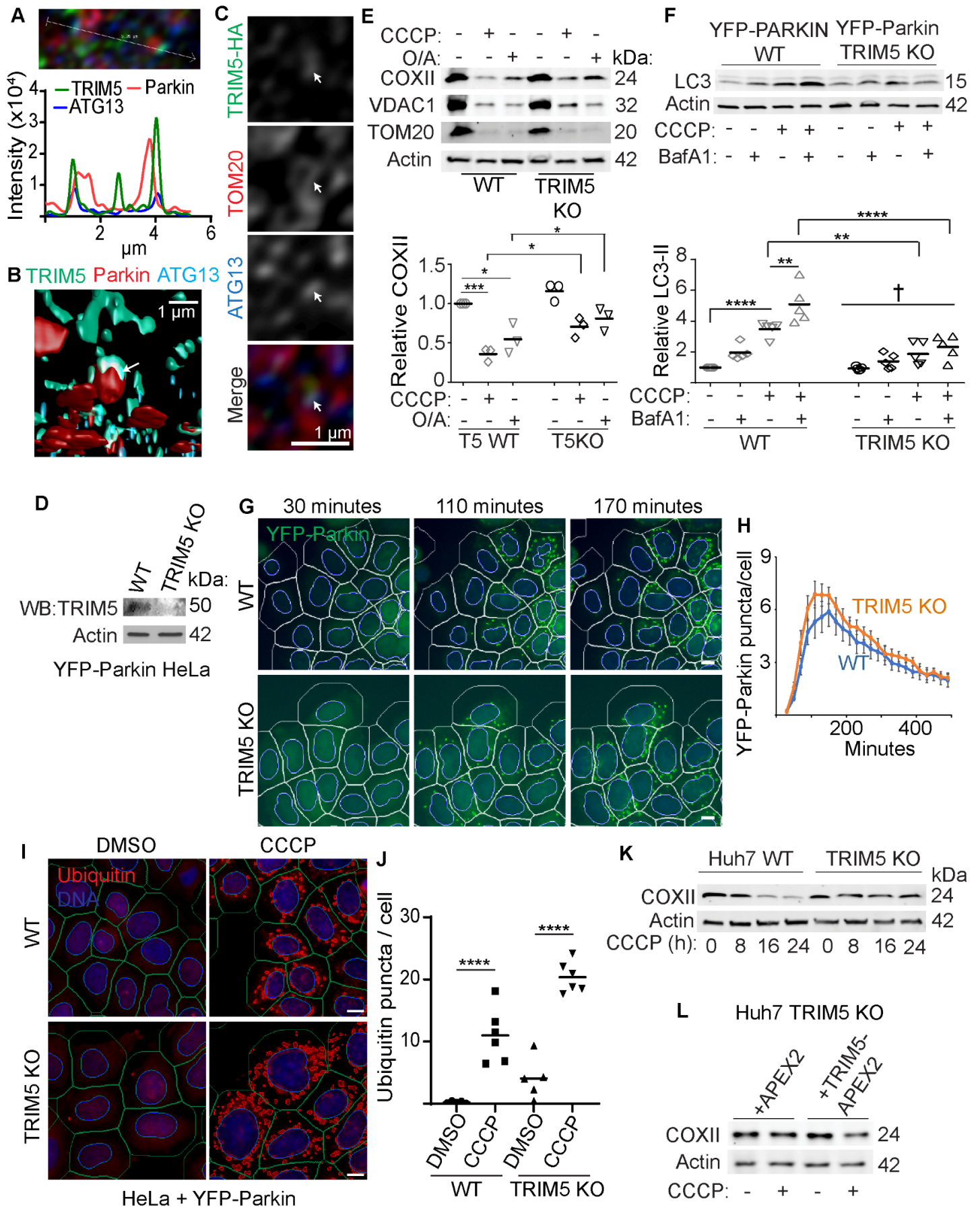
**Supplementary Figure S1. Identification of TRIM5-proximal proteins by mass spectrometry and immunoprecipitation. Related to Figure 1. (A)** Immunoblot analysis of APEX2-V5 or TRIM5-APEX2-V5 expression in stably transduced HEK293T cells.

**(B,C)** High content imaging based analysis of HIV restriction in APEX2-V5 expressing cell lines. The indicated stably transduced cell line was exposed to different dilutions of VSV-G pseudotyped HIV-1 encoding a GFP reporter. 2 days post infection, cells were fixed and stained with Hoechst 33342. Cells were automatically identified by nuclear staining and the above-background GFP intensity was measured per cell. N = 6 replicates with > 500 cells per replicate analyzed. **(D, E)** Impact of TRIM5-APEX2 expression on NF- $\kappa$ B and AP1 signaling in HEK293T cells transfected with plasmids encoding firefly luciferase under the control of NF- $\kappa$ B- or AP1-responsive promoters, constitutively active *Renilla* luciferase, and either TRIM5-APEX2 or APEX2 alone. 40-48h after transfection, samples were harvested, and luciferase values determined. N=3 biological replicates. **(F)** Principle component analysis of proteomic data from cells stably expressing rhesus TRIM5-APEX2-V5 (T5) or APEX2-V5 alone (AP2) and infected with VSV-G pseudotyped HIV-1 (HIV) or not (mock) for 3 hours prior to sample preparation. Shaded regions show 95% confidence ellipses. **(G)** Scatter plot of proteomic data from RhTRIM5-APEX2-V5 expressing cells infected or not with VSV-G. Dashed 45° line indicates no difference between samples. **(H)** Coimmunoprecipitation analysis of interactions between TRIM5 and selected proteins identified as TRIM5 proximal in mass spectrometry data from HeLa cells stably expressing HA-tagged human TRIM5. Control, immunoprecipitation with control IgG. N=2 biological replicates. **(I)** Summary of coimmunoprecipitation results from data shown in this figure and throughout the manuscript. All proteins tested were identified as being enriched in TRIM5-APEX2 datasets. Lysates from HeLa cells stably expressing TRIM5-HA were subjected to immunoprecipitation with anti-HA and immunoblots probed with the indicated antibodies (top matrix) or immunoprecipitated with the antibodies indicated in the middle and bottom matrices and immunoblots probed with anti-HA. Data: mean  $\pm$  SEM analyzed using two-way ANOVA or Student's t test; \*\*\*\*,  $P < 0.0001$ .



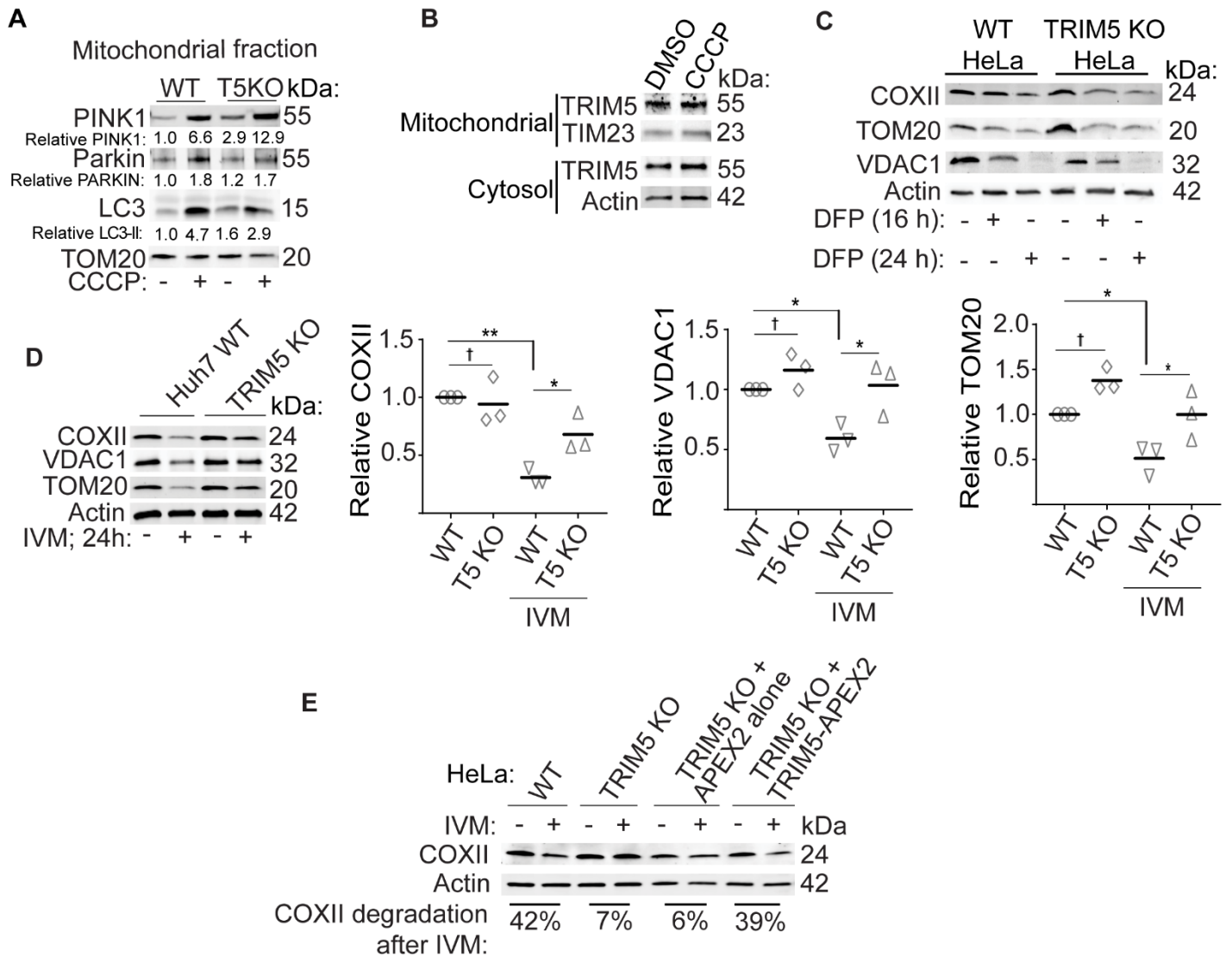
**Supplementary Figure S2. Localization of TRIM5 in cells following mitochondrial uncoupling with CCCP. Related to Figure 3.** HeLa cells stably expressing TRIM5-HA were transiently transfected with mCherry-tagged Parkin and treated with 20  $\mu\text{M}$  CCCP for 2 h prior to fixation. **(A)** 3D reconstruction of cells stained with antibodies recognizing HA. Zoomed in images of the region demarcated by the dashed line box are shown below. Each image shows the same structures from different viewpoints in X, Y, and Z planes. Voxels showing overlapping TRIM5 and Parkin signal are indicated by the gold color. **(B)** Morphological analysis of TRIM5 structures. HeLa cells were transiently transfected with GFP-TRIM5 and either mCherry or mCherry-Parkin prior to treatment with CCCP or DMSO control. Images show maximum image projections of representative transfected cells. The GFP-TRIM5 signal from the boxed regions is shown in the zoomed-in images below. GFP-TRIM5 structures were segmented and identified using Huygens image analysis software, which compared the volume of the structures with the volume of a hypothetical sphere having the same diameter as the observed structure. Thus, a perfectly spherical object would show a sphericity value of 1, with the sphericity decreasing as the structure's shape becomes more filamentous.  $N > 800$  GFP-TRIM5 structures. Data: \*\*\*\*,  $P < 0.0001$  by Kruskal Wallis. **(C)** Deconvolved confocal image of a CCCP-treated cell stained to detect TRIM5-HA, TOM20, and mCherry-Parkin. Zoomed in images of the boxed region are shown below. Arrow indicates a TRIM5-HA positive mitochondrion that is negative for mCherry-Parkin. **(D)** Confocal image of a CCCP-treated TRIM5-HA and mCherry-Parkin expressing HeLa cell stained with fluorescently-labeled phalloidin to detect filamentous actin. Zoomed-in images of the boxed region are shown below. Arrow indicates a TRIM5 filament that is adjacent to Parkin-positive mitochondria that is not detected with phalloidin. **(E)** Intensity profile showing triple colocalization of TRIM5-HA, mCherry-Parkin, and Calnexin in a CCCP-treated HeLa cell. The same cell was shown in Figure 3D. **(F-G)** Proximity ligation assay (PLA) probing the proximity of TRIM5-HA and the ER marker Calnexin in untreated cells (F) or

in CCCP-treated cells (G). Micrographs show representative confocal images. Plots show data from high content imaging in which both the number of PLA puncta and the total cross-sectional area of PLA puncta were measured per cell.  $N > 5000$  cells per treatment.



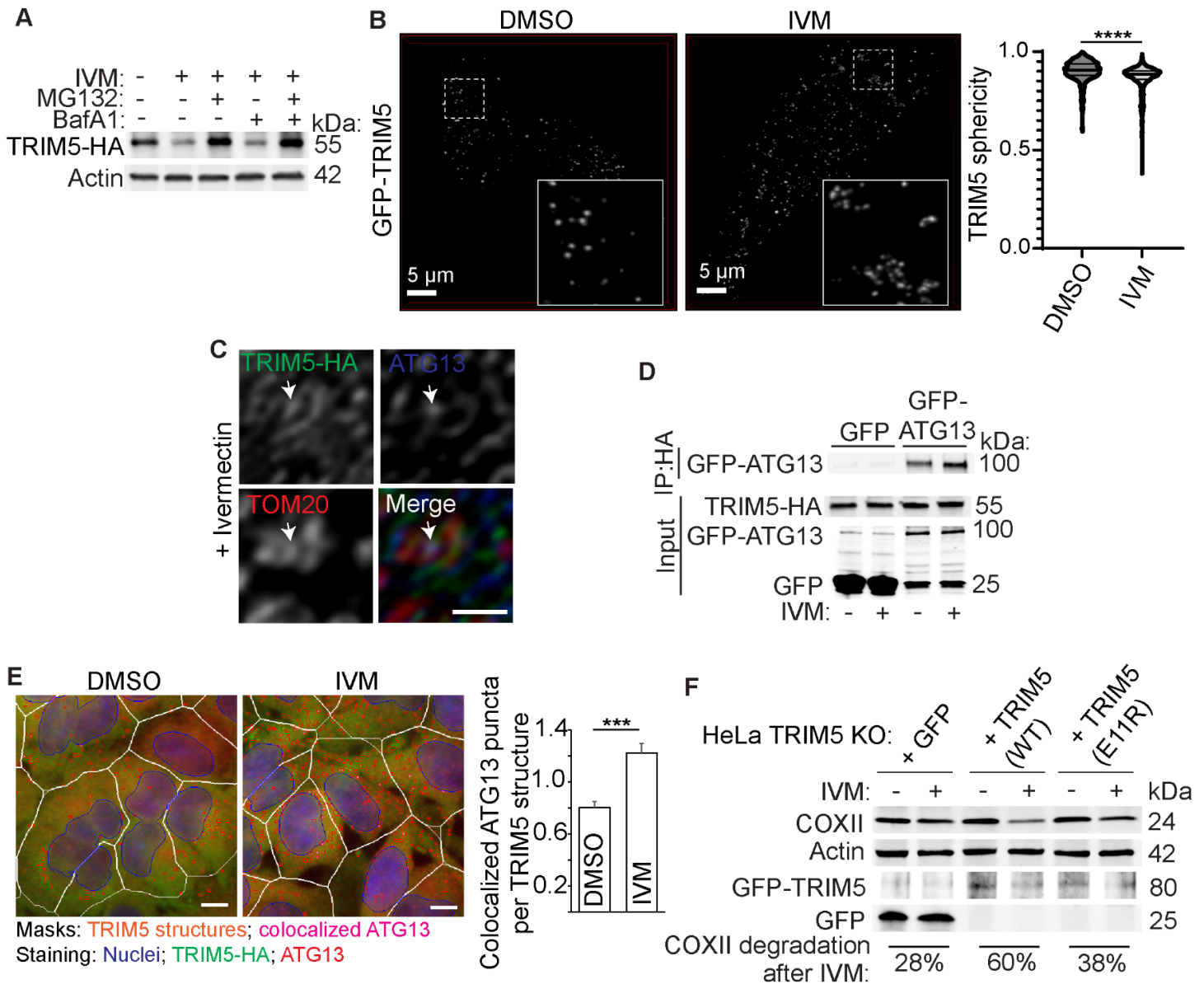
**Supplementary Figure S3. Impacts of TRIM5 on Parkin-dependent mitophagy. Related to Figure 4. (A)** Intensity profile from a deconvolved confocal image of a cell stained to detect TRIM5-HA (green), mCherry-Parkin (red), and endogenous ATG13 (blue) showing colocalized TRIM5 and ATG13 signals at specific foci on mCherry-Parkin positive mitochondria following a 2 hour

treatment with CCCP. **(B)** 3D reconstruction of a cell stained as in (A). Arrow indicates a TRIM5-ATG13 double-positive region on the outer face of a Parkin-positive mitochondrion. **(C)** Localization of TRIM5 to ATG13-positive foci on mitochondria does not require Parkin. HeLa cells stably expressing TRIM5-HA (but not transfected with Parkin) were treated with CCCP for 3 hours prior to fixation and staining with antibodies recognizing HA, TOM20, and ATG13. Image shows a deconvolved confocal image. Arrow indicates colocalized TRIM5 and ATG13 signal on the outside of a mitochondrion. **(D)** Immunoblot analysis of TRIM5 knockout efficiency in HeLa cells that stably express YFP-Parkin. **(E)** Immunoblot analysis of the effect of CCCP or oligomycin/antimycin (O/A) treatment on the abundance of mitochondrial proteins in WT and TRIM5 knockout HeLa cells that stably express YFP-Parkin. N = 3 independent experiments. **(F)** Immunoblot analysis of the impact of TRIM5 knockout on CCCP-induced autophagy in YFP-Parkin expressing HeLa cells treated or not with Bafilomycin A1 (BafA1). N = 5 independent experiments. **(G, H)** Time-lapse high content imaging analysis of YFP-Parkin puncta abundance in WT and TRIM5 knockout cells following treatment with 20  $\mu$ M CCCP for the indicated time points. Blue ring and white rings in E, automatically generated nuclear and cell boundary masks. Yellow mask, machine-identified YFP-Parkin puncta. N = 6 independent experiments with >500 cells analyzed per experiment. Scale bar, 20  $\mu$ m. **(I, J)** High content imaging and analysis of the abundance of ubiquitin puncta in WT and TRIM5 KO HeLa cells expressing YFP-Parkin and treated or not with 20  $\mu$ M CCCP for 3 hours. I, representative images of cells stained to detect poly-ubiquitin (red) and DNA (blue). Blue and green rings show automatically masked nuclear and cellular boundaries. Red mask indicates coalesced ubiquitin bodies identified within the cytoplasm. Scale bar, 20  $\mu$ m. N = 5 experiments with >500 cells analyzed per experiment. **(K)** Immunoblot analysis of COXII expression in WT and TRIM5 KO Huh7 cells following CCCP treatment for the indicated amount of time. **(L)** The impact of CCCP treatment on the abundance of the mitochondrial protein COXII in TRIM5 knockout Huh7 cells in which APEX2-tagged TRIM5 (human) had been reintroduced by lentiviral transduction. Transduction with an APEX2-alone expressing lentivirus was used as a negative control. Data: mean + SEM; *P* values determined by ANOVA, \*, *P* < 0.05; \*\*, *P* < 0.01; \*\*\*, *P* < 0.001; \*\*\*\*, *P* < 0.0001, †, not significant.

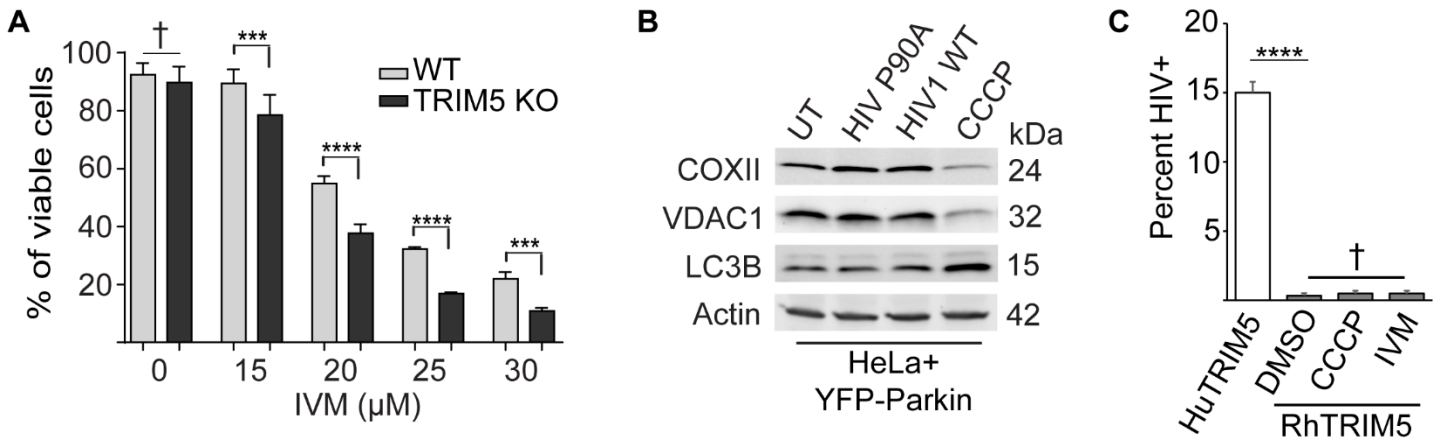


**Supplementary Figure S4. The role of TRIM5 in multiple mitophagy pathways. Related to Figure 5. (A)** WT or TRIM5 knockout Huh7 cells were treated or not with CCCP for 6 hours prior to harvest and mitochondrial fractionation. Lysates from purified mitochondria were subjected to immunoblotting with the indicated antibodies. Numbers indicate the relative abundance of the protein normalized to TOM20. **(B)** Huh7 cells were treated or not with CCCP for 6 hours in the presence of MG132 prior to mitochondrial fractionation and immunoblotting with the indicated antibodies. **(C)** Immunoblot analysis of the impact of DFP on the abundance of the indicated mitochondrial proteins in whole cell lysates from WT and TRIM5 knockout HeLa cells. Actin is used as a loading control. **(D)** Immunoblot analysis of the effect of ivermectin (IVM) treatment on the abundance of mitochondrial proteins in WT and TRIM5 knockout Huh7 cells. Cells were treated with IVM for 24 hours prior to lysis and immunoblotting with the indicated antibodies. Plots, the abundance of mitochondrial proteins COXII, VDAC1, and TOM20 was determined relative to actin. N = 3 independent experiments. **(E)** The impact of IVM treatment on the abundance of COXII in WT and TRIM5 knockout HeLa cells stably expressing HuTRIM5-APEX2 or APEX2 alone. Percentages represent the amount of COXII (relative to actin loading control) lost after IVM treatment for each cell line. Data: mean + SEM; P values determined by ANOVA, \*,  $P < 0.05$ ; \*\*,  $P < 0.01$ .





**Supplementary Figure S5. TRIM5 recruits the autophagy machinery to mitochondria damaged by ivermectin. Related to Figure 6.** (A) Immunoblot analysis of the abundance of TRIM5-HA in HeLa cells following treatment with IVM (15 μM, 4 hours) or vehicle control in the presence or absence of the indicated inhibitors. N=2 biological replicates. (B) Impact of IVM treatment on the shape of GFP-TRIM5 structures in HeLa cells. N > 850 GFP-TRIM5 structures. Data: median and quartiles shown; \*\*\*\*,  $P < 0.0001$  by Mann-Whitney. (C) Localization analysis of TRIM5-HA, ATG13, and TOM20 in HeLa cells following 2 h ivermectin treatment. Arrow indicates a site on a mitochondrion to which both TRIM5 and ATG13 localize. (D) Coimmunoprecipitation analysis of interactions between GFP-ATG13 and TRIM5-HA in HeLa cells treated with MG132 in the presence or absence of IVM for 4 hours. (E) High content imaging based determination of spatial relationships between TRIM5-HA and endogenous ATG13 in HeLa cells treated or not with IVM for 6 hours. Cells were automatically imaged and the number of ATG13 puncta showing overlap with TRIM5-positive structures was determined. N=6 biological replicates. Scale bar, 10 μm. (F) The impact of expressing WT or E11R TRIM5 (GFP-tagged) on restoring IVM-triggered mitophagy in TRIM5 knockout HeLa cells. Data: mean + SEM by Student's t test, \*\*\*,  $P < 0.001$ ; \*\*\*\*,  $P < 0.0001$ .



**Supplementary Figure S6. TRIM5-dependent mitophagy is independent of TRIM5 actions in HIV restriction. Related to Figure 7. (A)** AlamarBlue-based assessment of cell viability in WT and TRIM5 knockout Huh7 cells following 24 h treatment with the indicated concentrations of IVM. N=6 biological replicates. **(B)** The impact of infection with TRIM5-sensitive (HIV P90A) or TRIM5-resistant (HIV WT) pseudoviruses on mitochondrial protein abundance and on LC3B conversion in HeLa cells expressing YFP-Parkin. Cells were subjected to synchronous infection with VSV-G pseudotyped HIV for 24 hours prior to lysis and immunoblotting with the indicated antibodies. CCCP treatment (24 hours) was used as a positive control for mitophagy induction. **(C)** The impact of mitophagy-inducing compounds on the ability of RhTRIM5 to restrict HIV-1. HeLa cells stably expressing HuTRIM5 or RhTRIM5 were infected with VSV-G pseudotyped HIV-1 encoding a GFP reporter after 1.5 hours pre-treatment with CCCP, IVM, or DMSO control. Virus was then allowed to enter cells for 4 h in the presence of the compounds, after which the media was replaced. 48 h later, the percent of cells showing GFP positivity was determined by high content imaging. N=6 biological replicates. Data: mean + SEM; *P* values determined by ANOVA, \*\*\*, *P* < 0.001; \*\*\*\*, *P* < 0.0001; †, not significant.